American Mineralogist, Volume 67, pages 865–876, 1982

A petrogenetic grid for medium and high grade metabasites

RICHARD N. ABBOTT, JR.

Department of Geology
Appalachian State University
Boone, North Carolina 28608

Abstract

Inspired by phase relationships in the Precambrian Ashe Formation of northwest North Carolina, a petrogenetic grid is presented for metabasites containing quartz, feldspar, magnetite and one or more of the minerals hornblende, biotite, garnet, epidote, orthopyroxene, clinopyroxene and fayalite. The applicable range of conditions is from the amphibolite facies to the granulite facies. There are 26 subfacies in the grid, each represented by a distinct CFM topology (C = CaO–Al_2O_3 + Na_2O + K_2O, F = FeO–Fe_2O_3, M = MgO). Construction of the grid was guided by natural mineral assemblages. Some of the subfacies, particularly at low pressures, have not been identified in natural assemblages.

Many of the subfacies represent conditions under which melting may occur. The possibilities for melting are explored in the context of previous work by the writer (Abbott and Clarke, 1979; Abbott, 1981). The analysis shows that anatexis of high grade metabasites may produce distinctly peraluminous, granitic liquids.

Introduction

Metamorphic subfacies are not easily distinguished in metabasites of the amphibolite facies and granulite facies. In some terranes, variations in the grade of metamorphism can be determined only by careful chemical analyses of the coexisting minerals in selected assemblages occurring over a wide area. Part of the problem is that there is no well-established and convenient chemographic means of representing subfacies of the facies defined, for instance, on the basis of Eskola's (1939) ACF diagram (A = Al_2O_3 + Fe_2O_3–Na_2O–K_2O, C = CaO, F = MgO + FeO). There is no satisfactory way of handling metabasite mineral assemblages, *e.g.*, in a manner like Thompson's (1957) AFM diagram for metapelites (A = Al_2O_3–K_2O, F = FeO, M = MgO, projected from alkali feldspar), for the purpose of representing mineral assemblages, and predicting and recognizing reactions.

There are three objectives in the paper. The first objective is to present an extended version of Thompson's (1957) AFM diagram, redesigned to accommodate observed metabasite mineral assemblages from medium and high grade metamorphic terranes. The second is to propose a qualitative *P–T* petrogenetic grid for such metabasites based on natural mineral assemblages. The third and last objective is to examine the consequences of anatexis in high grade metabasites.

This paper was inspired by a preliminary investigation of the late Precambrian Ashe Formation in the Blue Ridge Province of northwestern North Carolina, an investigation in which I experienced difficulties in comparing the observed mineral assemblages with the metamorphic facies in other terranes.

The Ashe Formation (Rankin *et al.*, 1973) in northwest North Carolina consists of amphibole gneisses and schists interlayered with lesser amounts of quartz-feldspar gneisses and micaceous schists. The amphibolites contain hornblende and plagioclase with various combinations of quartz, magnetite, garnet, epidote, biotite, alkali feldspar and sulfides. This investigation focuses on the amphibolites with quartz, magnetite, alkali feldspar and combinations of garnet, epidote and biotite. The amphibolites are interpreted as metabasalts (Rankin *et al.*, 1973). Most of the ultramafic rocks in the Blue Ridge Province are associated with the Ashe Formation or with rocks presumed to be correlative with the Ashe Formation. The Ashe Formation is structurally underlain by older quartz-feldspar gneisses of the Cranberry Gneiss and

0003–004X/82/0910–0865$02.00

grades upward into later Precambrian, possibly lower Paleozoic, micaceous schists of the Alligator Back Formation.

The CFM projection

One of the main problems in the graphical representation of mineral assemblages in metabasites is the common occurrence of more minerals than can be conveniently accommodated in two dimensions. Even by projecting the mineral assemblages from one or more minerals, the problem of crossing tielines commonly persists. This is most apparent in the classical ACF diagram (Eskola, 1939; Turner, 1948; Winkler, 1965) so commonly used to represent mineral compatibilities for a wide range of bulk compositions. In the ACF diagram, epidote (Epi) and plagioclase (Pla) are common in assemblages also containing two or more of the other ACF minerals, hornblende (Hnb), garnet (Gar), clinopyroxene (Cpx), orthopyroxene (Opx), biotite (Bio) and olivine (fayalite = Fay). The ACF diagram is not adequate for representing even the most common assemblages. Both Turner (1948) and Winkler (1965) recognized this problem. For facies containing both plagioclase and epidote, these minerals are usually enclosed in brackets on the ACF diagram. What is meant is that both minerals may occur with one, two or more of the other ACF minerals.

Another disadvantage of the ACF diagram is the treatment of MgO and FeO as one component (F = FeO + MgO). Important changes in mineralogy are commonly due to changes in the FeO/MgO ratio of the minerals in various assemblages. Admittedly, the ACF diagram has been used to great advantage in correlating grades of metamorphism for very different bulk compositions. This is its principle value.

A useful projection would incorporate features of the AFM projection, most importantly a means of discriminating minerals on the basis of FeO/MgO. Of course, some information is lost when projecting from minerals which are not variable in FeO/MgO, but variable in other components. In the case of the AFM diagram, compositions are projected from quartz (Qtz), H_2O, muscovite or alkali feldspar (Ksp), or in some applications quartz, H_2O, alkali feldspar and plagioclase. Except for muscovite, these same minerals are very common in metabasites in the amphibolite facies and granulite facies. For certain applications the AFM diagram is well suited for representing some metabasite mineral assemblages (Reinhardt and Skippen, 1970). With the exception of garnet and biotite, the metabasite minerals are metaluminous or subaluminous and appear in the AFM projection where A is zero or negative. This minor inconvenience is easily rectified by plotting the negative of $A = C = CaO + Na_2O + K_2O - Al_2O_3$, where the compositions are projected from quartz, H_2O, and the feldspar components. The CFM diagram shows the metaluminous and subaluminous compositions inside the triangle defined by C, F and M, where C is positive; with the peraluminous (pelitic) part of the diagram outside the triangle, where C is negative. This representation, or a similar one, has been used in a number of investigations (Klein, 1968; Robinson and Jaffe, 1969; Harte and Graham, 1975).

A preliminary investigation of the metabasites in the late Precambrian Ashe Formation in North Carolina has shown that magnetite is an important "saturating" mineral. Systematic differences in the mineral assemblages, reflecting differences in the grade of metamorphism, are not at all apparent, unless the presence or absence of magnetite is taken into account. Different grades of metamorphism, separated by CFM reaction isograds, can be recognized only in the class of metabasites containing magnetite (+ Qtz + Pla±Ksp). When magnetite is ignored, the distribution of CFM mineral assemblages shows no systematic variation, and the CFM assemblages cease to be useful in discriminating different grades of metamorphism. For this reason and because observations of the Ashe Formation prompted this paper, a slightly modified version of the CFM diagram is used (Fig. 1) in which compositions are projected from quartz, H_2O, the feldspar components and magnetite onto the CaO(C)–FeO(F)–MgO(M) plane in the system SiO_2–MgO–FeO–Fe_2O_3–K_2O–Na_2O–CaO–Al_2O_3–H_2O. For plotting purposes, the CFM parameters are figured as $C = CaO + K_2O + Na_2O - Al_2O_3$, $F = FeO - Fe_2O_3$ and M = MgO. The important mineral compositions are shown in Figure 1. All of the minerals in Figure 1 except epidote lie approximately in the CaO–FeO–MgO plane. Epidote contains ferric iron and projects onto the CF join where F is negative, $F/(C + F) = -1$.

The order of $X_F = F/(M + F)$ for some coexisting pairs of CFM minerals is X_F(Opx) > X_F(Hnb), X_F(Hnb) > X_F(Cpx) (Spear, 1981; Engel and Engel, 1962; Jan and Howie, 1981), X_F(Gar) > X_F(Hnb) (Jan and Howie, 1981; Laird, 1980), X_F(Gar) > X_F(Bio) (Albee, 1965; Ferry, 1978; Laird, 1980);

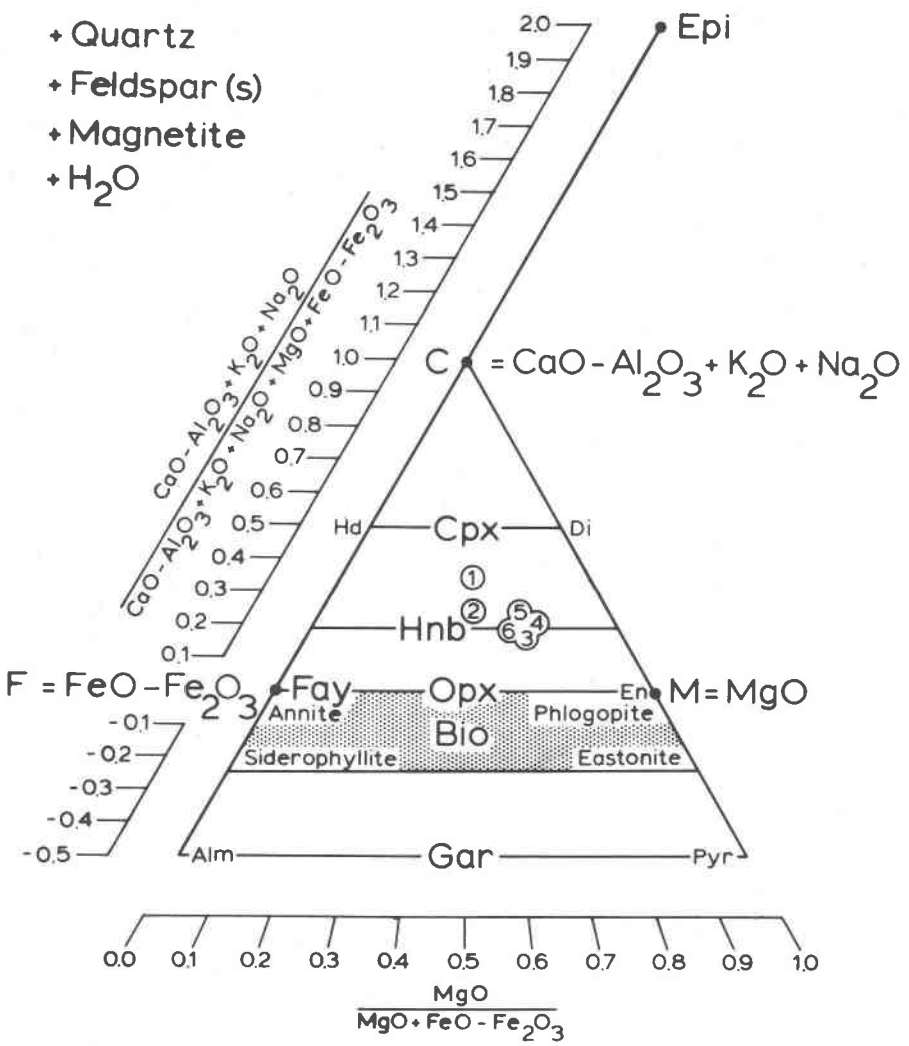

Fig. 1. The CFM diagram, showing the ranges of various mineral compositions projected from quartz, H_2O, the feldspar components and magnetite onto the CaO–FeO–MgO plane. Epi = epidote, Cpx = clinopyroxene (Hd = $CaFeSi_2O_6$, Di = $CaMgSi_2O_6$), Hnb = hornblende, Opx = orthopyroxene (En = $Mg_2Si_2O_6$), Fay = fayalite, Bio = biotite, Gar = garnet (Alm = $Fe_3Al_2Si_3O_{12}$, Pyr = $Mg_3Al_2Si_3O_{12}$). Also shown are 6 averaged basalt compositions; average (1) of 19 basalts (Benson, 1941), average (2) of 11 Deccan basalts (Washington, 1922), average (3) of 10 Oahu basalts (Wentworth and Winchell, 1947), average (4) of 24 Mauna Loa basalts (MacDonald, 1949), average (5) for oceanic basalts and average (6) for continental basalts (Ronov and Yaroshevsky, 1969).

$X_F(Gar) > X_F(Cpx)$, $X_F(Gar) > X_F(Opx)$ (Jan and Howie, 1981), $X_F(Opx) > X_F(Cpx)$ (Spear, 1981) and $X_F(Bio) > X_F(Hnb)$ (Laird, 1980). At high P and low T the partitioning of Fe and Mg between coexisting biotite and hornblende may be reversed, $X_F(Bio) < X_F(Hnb)$ (Laird, personal communication).

In the Ashe Formation two metamorphic subfacies are recognized on the basis of the mineral assemblages (Fig. 2), and numbered according to Figure 3:

Subfacies 6 (or 5)
(Qtz + Mgt + Pla±Ksp) + Hnb + Bio + Epi
+ Hnb + Bio
+ Hnb + Epi
+ Hnb

Subfacies 7 (or 9)
(Qtz + Mgt + Pla±Ksp) + Hnb + Gar + Epi
+ Hnb + Gar + Bio
+ Hnb + Gar
+ Hnb

A third subfacies may exist, characterized by the

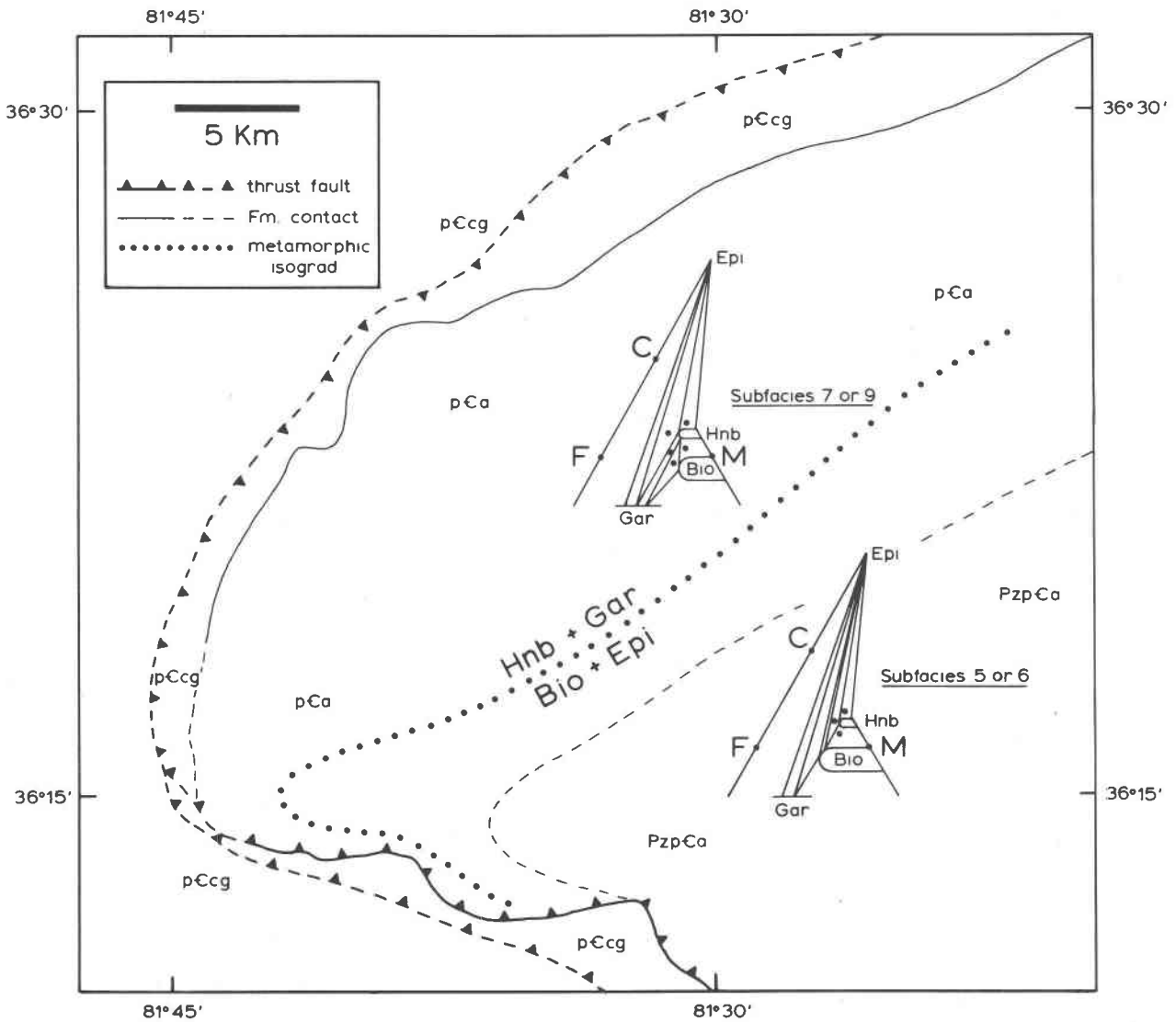

Fig. 2. Geological map of part of northwestern North Carolina (after Rankin *et al.*, 1972, 1973) showing the Ashe Formation (pCa, mostly amphibole schists and gneisses) and the metamorphic isograd, reaction (Cpx, Fay, Opx), separating subfacies 5 (or 6) from subfacies 7 (or 9). pCcg = Cranberry Gneiss (mostly quartz-feldspar gneisses), PzpCa = Alligator Back Formation (mostly mica schists).

presence of clinopyroxene (Jones, 1973), but this was not confirmed in the present investigation. Subfacies 6 (or 5) and 7 (or 9) are separated by an isograd marking the CFM reaction (and see Figure 2):

$$\text{Bio} + \text{Epi} = \text{Gar} + \text{Hnb} \qquad (1)$$

This reaction and others in this paper are reported in terms of the CFM minerals only. Quartz, feldspars, magnetite and an aqueous phase are involved as necessary to balance the reactions.

Petrogenetic grid

In an attempt to compare the metamorphic subfacies in the Ashe Formation with the subfacies of metabasites in other areas, the petrogenetic grid of Figure 3 was constructed in two stages. In the first stage, Schreinemakers' analysis (*e.g.*, see Korzhinskii, 1957) in conjunction with natural mineral assemblages, from all over the world and described principally in Dobretsov *et al.* (1973), were used to establish the relationships between the stable (naturally occurring) mineral assemblages involving Fay,

Bio, Opx, Cpx, Gar and Hnb. Epidote was not considered at this stage. The important mineral assemblages cluster around the invariant point designated [Fay, Epi] where the square brackets indicate the invariant point for univariant reactions not involving fayalite and epidote. The univariant reactions are designated in a similar fashion, but using parentheses instead of square brackets, hence reaction 1 is (Cpx, Fay, Opx). Fayalite is included in the analysis because it is compatible with quartz, feldspar and magnetite in high F/M bulk compositions (Eugster, 1956; Eugster and Wones, 1962).

The reactions represented in terms of the 3 CFM components involve combinations of four of the six minerals, Hnb, Cpx, Opx, Bio, Gar and Fay. The phase rule dictates 15 univariant reactions and 6 invariant points, all shown in Figure 3a. The 6 invariant points are [Fay, Epi], [Bio, Epi], [Cpx, Epi], [Hnb, Epi], [Opx, Epi] and [Gar, Epi]. Most of the CFM topologies around the points [Fay, Epi] and [Bio, Epi] are represented by natural assemblages indicated by dots in the various CFM diagrams (Fig. 3b). This is interpreted as partial confirmation of the first stage of analysis. Several of the topologies surrounding points [Fay, Epi] and [Bio, Epi] are consistent with 3-mineral CFM assemblages of the upper amphibolite facies and granulite facies depending on the bulk CFM composition. In fact, practically all of the natural mineral assemblages reported in the CFM diagrams around point [Fay, Epi] come from granulite terranes. High temperature eclogite-like assemblages (Group B eclogites of Coleman *et al.*, 1965) are presumed to be at least possible over wide ranges of P, but in nature, largely restricted to high pressures because of the high bulk ratio of M/F in the majority of metabasites. The appearance of orthopyroxene is interpreted in the simplest way possible consistent with the natural mineral assemblages, as the result of one of four 4-mineral terminal-type CFM reactions, (Cpx, Epi, Fay), (Epi, Fay, Hnb), (Cpx, Gar, Hnb) or (Cpx, Fay, Hnb). The last two reactions involve epidote and are suggested on the basis of the second stage of analysis. The possibility that the low temperature stability limit for orthopyroxene is some 3-mineral CFM colinearity (*e.g.*, Gar + Hnb = Opx) was considered and deemed unlikely because of the lack of documentary natural assemblages and Occam's razor. If orthopyroxene is involved in a colinearity, parts of the grid become much more complicated, so as to defy reasonable testing (in my opinion).

The second stage of analysis incorporates reactions involving epidote. On the basis of the phase rule, with the addition of epidote, there are 35 univariant reactions and 21 invariant points in the system. It should be noted that, as dictated by Schreinemakers' analysis and the phase rule, there are three invariant points on each univariant reaction. Only those reactions and invariant points believed to be stable are shown in Figure 3. Metabasite mineral assemblages in the low grade part of the amphibolite facies pass into the high grade part of the amphibolite facies by way of two reactions. The reactions, defined on the basis of naturally occurring assemblages such as those in the Ashe Formation, are

$$\text{Bio} + \text{Epi} = \text{Gar} + \text{Hnb}\ (\text{Cpx, Fay, Opx}) \quad (1)$$

$$\text{and Gar} + \text{Epi} = \text{Cpx} + \text{Hnb}\ (\text{Bio, Fay, Opx}) \quad (2)$$

These reactions meet at the invariant point [Fay, Opx] and give rise, by way of Schreinemakers' analysis, to the points [Fay, Cpx], [Cpx, Bio], [Opx, Bio], [Hnb, Opx], [Hnb, Cpx] and [Bio, Gar]. In the upper part of the diagram (moderately high pressure, as will be shown) the various CFM topologies are fairly well represented by the natural assemblages. High F/M metabasites or other possible fayalite-bearing rock types (*e.g.*, some iron formations, some granites) are rare, so that reactions involving fayalite are not well documented. The lower part of Figure 3 (low pressures) is not well documented for much the same reason, but some assemblages involving fayalite do occur in hypabyssal granites and some volcanic rocks (Oyawaye and Makanjaola, 1972; Bacon and Duffield, 1981).

All reactions in which H_2O is believed to be involved on the high temperature side of the reaction (dehydration with prograde metamorphism) are shown with positive P–T slopes in Figure 3. The reaction (Gar, Hnb, Opx) may involve H_2O on the low temperature side of the reaction (hydration with prograde metamorphism) and, for this reason, is shown with a negative slope. As a consequence of the ordering of the stable and metastable parts of reactions around invariant points [Hnb, Opx], [Fay, Opx] and [Fay, Epi], reactions (Fay, Hnb, Opx), (Epi, Fay, Opx) and (Epi, Fay, Gar) would also have negative slopes. The slope of reaction (Bio, Epi, Hnb) is ill-defined because the reaction is anhydrous.

For the medium and high grades of metamorphism discussed in this paper a second amphibole,

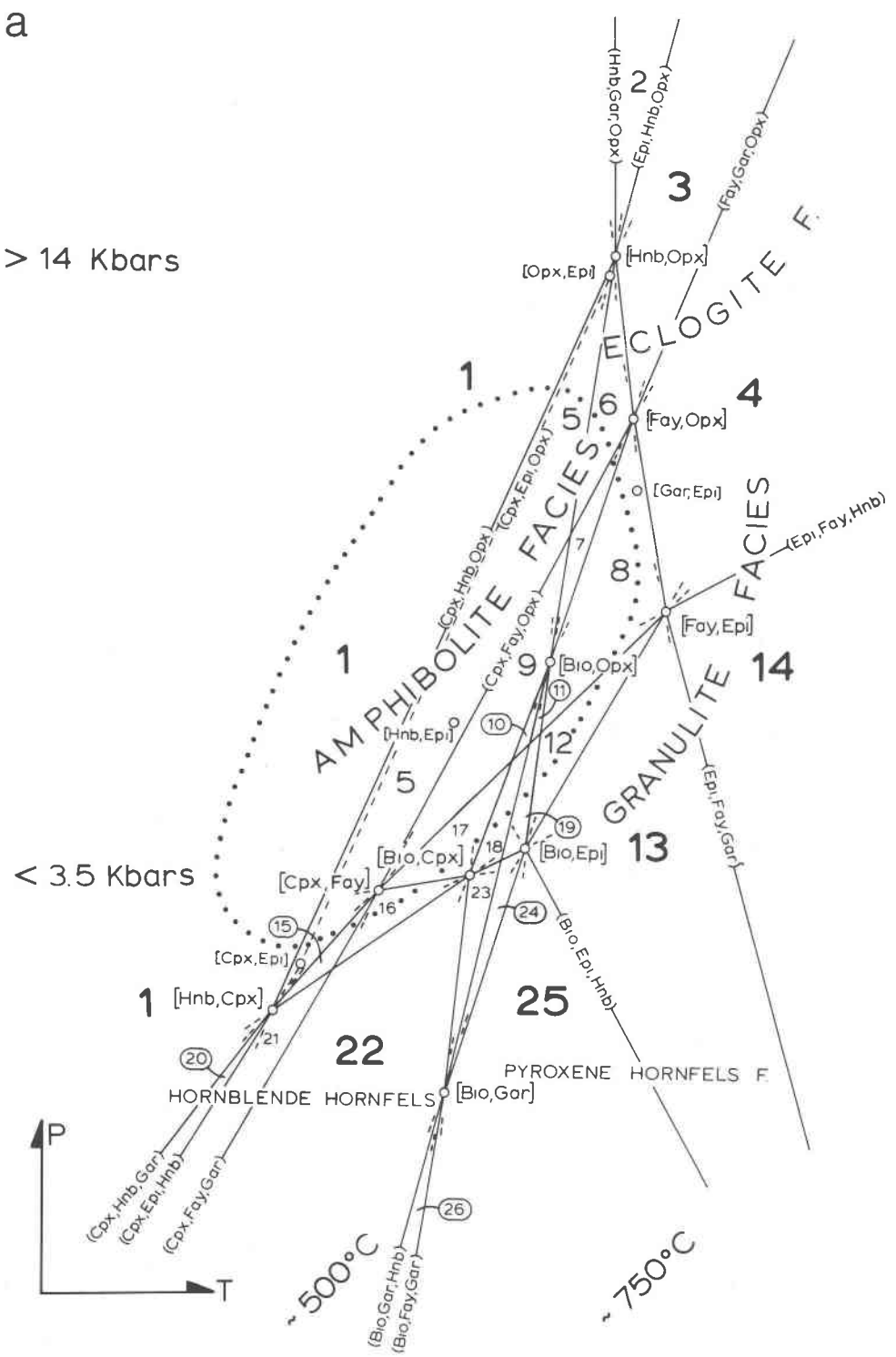

Fig. 3. Schematic petrogenetic grid and CFM topologies for amphibolite facies and granulite facies metabasites. a. The petrogenetic grid. There are 26 subfacies. b. (See next page.) Each subfacies is characterized by a distinct CFM topology. Observed assemblages of 3 CFM minerals are shown by dots in the various CFM topologies. The sources for the observed mineral assemblages are Dobretsov *et al.* (1972), Engel and Engel (1962), Windley (1970), Oyawaye and Makanjaola (1972), Bacon and Duffield (1981), Jan and Howie (1981), Johannsen (1939) and Reinhardt and Skippen (1970).

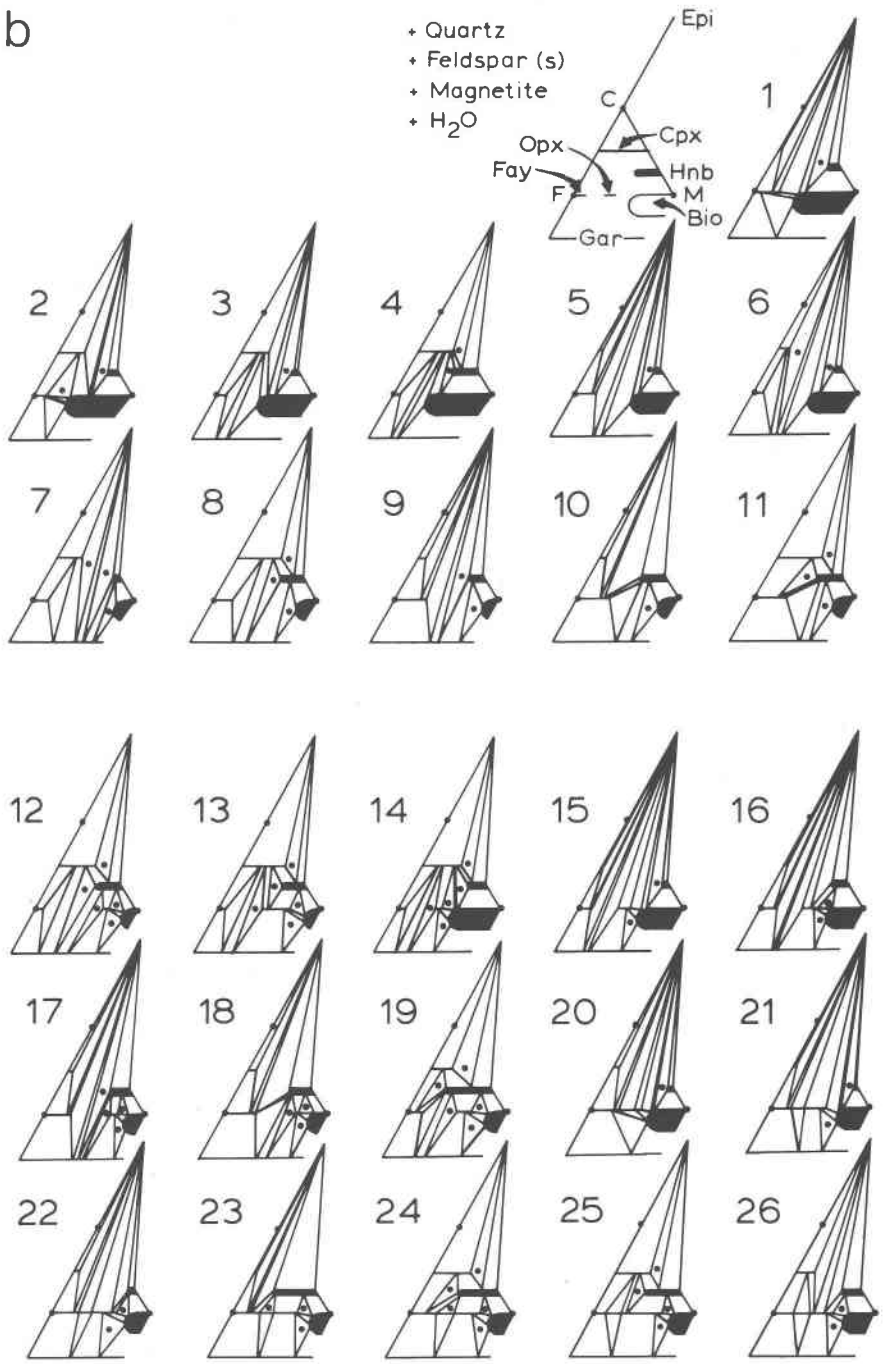

such as actinolite (Harte and Graham, 1975; Laird, 1980), is unlikely in the presence of quartz. This is evident in the natural assemblages reported in Figure 3b where the only amphibole is a variety of common hornblende. The composition of the hornblende depends on the coexisting minerals. It may be inferred from Figure 1 that hornblende is somewhat aluminous where coexisting with garnet, biotite or both, and low in aluminum where coexisting with clinopyroxene, epidote or both.

Hornblende and biotite can be stable at substantially higher temperatures than the presumed applicable range of temperatures for Figure 3. The magnesian hornblende, pargasite, is stable at temperatures higher than 950°C for pressures above 1 kbar (Ernst, 1968). Kushiro (1970) determined that

the P–T breakdown curve for hornblende has a maximum temperature just over 1000°C at a pressure of approximately 12 kbar. Phlogopite is stable at temperatures higher than approximately 1050°C for pressures above 1 kbar (Yoder and Eugster, 1956).

At the grades of metamorphism discussed in this paper, chlorite may still be stable but only in extremely high M/F bulk compositions. Ultramafic bodies in the Ashe Melange commonly have chlorite. In the metabasites, chlorite was not observed except as a secondary, possibly retrograde, replacement of the other minerals.

In Figure 3 there is no high temperature limit to the stability of epidote. Extrapolation of some of the recent experiments of Bird and Helgeson (1981, their Figures 10 and 22) suggests that epidote solid solution may be stable in the presence of quartz and feldspar to temperatures at least as high as 700°C at $P(H_2O) = P(\text{total}) = 5$ kbar, depending on the fugacity of oxygen and other factors related to the composition of the coexisting aqueous phase. Liou (1973) synthesized epidote in the presence of magnetite and quartz at temperatures as high as 750°C at 5 kbar and 680°C at 3 kbar. These conditions are consistent with granulite facies metamorphism, hence there is little reason to suspect that epidote ceases to be possible within the range of conditions represented by Figure 3. The problem is difficult to assess because the compatibility of Hnb + Cpx around the invariant points [Bio, Epi] and [Fay, Epi] precludes the occurrence of epidote in all but the most calcic bulk compositions. For this reason, at high temperatures in Figure 3, it is not surprising that epidote is rare or absent in the natural assemblages. Epidote disappears from the projection under conditions of low P and high T, outside the range of conditions intended for the petrogenetic grid. Even so, this may have little or no effect on the chemographic relationships since the epidote is simply replaced by grandite or grossular rich in ferric iron (Liou, 1973; Bird and Helgeson, 1981).

Abbott (1981) justified the reaction,

$$\text{Bio} + \text{Fay} = \text{Gar} + \text{Hnb} \quad (\text{Epi, Cpx, Opx}) \quad (3)$$

on the basis of natural mineral assemblages. This reaction is metastable in Figure 3 as a consequence of Schreinemakers' analysis. The CFM assemblage Fay + Gar + Bio, which is possible on the low temperature side of the reaction, was reported by Korzhinskii (1936) from pelitic rocks and more recently by Bacon and Duffield (1981) from felsic volcanic rocks. The assemblage is compatible with subfacies 1, 2 or 20. Korzhinskii's (1936) assemblage comes from rocks with practically no calcium. Even without calcium, the assemblage can still be referred to the CFM diagram. However, under these circumstances, epidote is not possible and the reported assemblage may persist, even in the presence of magnetite, to higher temperatures than subfacies 1, 2 and 20. Bacon and Duffield's (1981) assemblage does not occur with magnetite, even though this mineral does occur in other felsic volcanic mineral assemblages reported by them. It should be noted that quartz is not present. Bacon and Duffield (1981) argue that the activity of SiO_2 was close to one. If so, the CFM projection would be applicable, were it not for the absence of magnetite. Without magnetite, the assemblage Fay + Gar + Bio may persist at higher temperatures than subfacies 1, but not at higher temperatures than the reaction (Epi, Cpx, Opx) which limits the compatibility of biotite and fayalite in rocks with no magnetite or where the fugacity of oxygen is very low. Bacon and Duffield (1981) suggest that the activity of H_2O was less than one. This shifts the reaction (Cpx, Epi, Opx) to higher temperatures, expanding the region where biotite and fayalite can coexist.

High temperature Gar + Cpx assemblages in many terranes result from a shift to higher M/F of the various 3-phase regions in the CFM projection (Figure 3) as T, P or both are increased. The bulk composition, in particular F/M, may determine the appearance of the assemblage Gar + Cpx + Opx. This is illustrated by the prograde sequence of assemblages encountered in the Adirondacks of New York (Engel and Engel, 1962). Here, the sequence of assemblages is Hnb + Cpx, Hnb + Cpx + Opx, Opx + Cpx + Gar. The assemblages are consistent with one of the subfacies in Figure 3, CFM topology 13. The sequence of assemblages can be explained in the present context if the average bulk composition of the metabasites is the same everywhere in the affected area. The different assemblages result from a decrease in X_F of the minerals in the 3-phase CFM assemblages Hnb + Cpx + Opx and Cpx + Opx + Gar. The 3-phase regions shift to lower X_F. A bulk composition in the Hnb + Cpx field at low P, T or both, will, with increasing P, T or both, be situated successively in the different CFM fields, in order, Hnb + Cpx, Hnb + Cpx + Opx, Cpx + Opx, Cpx + Opx + Gar, Cpx + Gar.

Physical conditions

The CFM topologies in Figure 3 represent subfacies of the amphibolite facies and granulite facies. The range of temperatures for these facies is from approximately 500° C to 800° C; the range of pressures is from 1 bar to at least 10 kbar, (Turner, 1968; Winkler, 1979; Dobretsov *et al.*, 1972). The invariant points [Bio, Epi] and [Fay, Epi] divide the figure into three pressure regimes. The observed topologies at lower pressures than [Bio, Epi] are associated with hypabyssal intrusive rocks or volcanic rocks. One of the most frequently encountered topologies, subfacies 12, is restricted to pressures between [Bio, Epi] and [Fay, Epi]. The natural assemblages of subfacies 14 and 13 are commonly found near natural assemblages of subfacies 12, as in the Adirondacks and numerous other places cited by Dobretsov *et al.* (1972). Sillimanite is common in pelitic rocks associated with the metabasites. The topologies above [Fay, Epi] in Figure 3 represent high pressure compatibilities. In the case of the Ashe Formation high P is evident from the presence of kyanite in associated pelitic rocks. There are a great number of possible Cpx-bearing assemblages above [Fay, Epi], in particular Gar + Cpx, and this is considered to be consistent with high pressures.

The mineral pair Gar + Hnb is possible in a region enclosed by the reactions (Fay, Cpx, Opx), (Fay, Opx, Epi), (Fay, Epi, Bio), (Bio, Cpx, Epi) and (Cpx, Fay, Bio) which connect the invariant points [Fay, Opx], [Fay, Epi], [Bio, Epi], [Cpx, Bio] and [Fay, Cpx]. Ferry (1979) has encountered the CFM assemblage Gar + Hnb + Bio in granites from central Maine. The regional metamorphism is characterized by andalusite–sillimanite. Ferry (1979) estimates the conditions for the assemblage as 3.5 kbar and at least 650° C. Jan and Howie (1981) observed the CFM assemblages Cpx + Hnb + Gar, and Epi + Gar + Hnb in high grade metabasites in Pakistan. The assemblages are consistent with subfacies 7 and 8. The estimated conditions are 12 to 14 kbar, 670° to 690° C. (Jan and Howie, 1981). Assemblages containing Gar + Hnb are possible over a very wide range of pressures from less than 3.5 kbar to at least 14 kbar. These pressures are consistent with depths from less than 10 to greater than 40 km, the lower three-quarters of the average continental crust.

Melting possibilities

The petrogenetic grid of Figure 3 is only applicable for assemblages containing quartz, magnetite and plagioclase with or without an alkali feldspar. For the range of conditions represented by the grid, it is quite likely that a silicate liquid may appear. Many of the metabasites of the Ashe Formation are gneisses with thin layers rich in quartz and feldspar. Pegmatitic layers are also common. Except for the lowest pressures and temperatures, most of the subfacies in Figure 3 are well above the temperature of the H_2O-saturated minimum melting reaction for granites (Tuttle and Bowen, 1958). The silicate liquid would certainly dissolve at least small amounts of the CFM minerals (Abbott and Clarke, 1979; Abbott, 1981), hence the liquid will appear in the CFM projection. The addition of one new phase, the silicate liquid, greatly complicates the already complicated relationships of Figure 3. With 7 possible CFM minerals and the liquid, there are 70 univariant reactions and 56 invariant points. No attempt is made here to evaluate the possibilities, which will depend on the activity of H_2O among other factors.

An approach to the problem, applicable to metabasites containing quartz and feldspar, has been presented for pelitic rocks and some metaluminous rocks by Abbott and Clarke (1979) and Abbott (1981). The ideas presented in this section follow directly from these previous papers. That the melting of high grade metabasites may result in a granitic liquid is self-evident in the natural mineral assemblages. The main distinction between the most common metabasite assemblages in the Ashe Formation and granitic mineral assemblages is the relative proportions of the minerals. On the basis of the volume of the leucocratic partings in the gneissic metabasites of the Ashe Formation at least 5 to 10 percent granite liquid could be extracted without changing the mineral assemblage of the restite. I suspect the same is true elsewhere because quartz and one or two feldspars are very common in high grade metabasites (Dobretsov *et al.*, 1973). Metabasites may be the dominant rock type in the lower part of continental crust (Kay and Kay, 1981) where crustal anatexis is most likely to occur. Even though the metabasites are generally strongly metaluminous, the first silicate liquid formed upon melting is quite likely to be peraluminous (Abbott, 1981).

Hornblende is by far the most abundant mineral in the metabasites of the Ashe Formation. The other CFM minerals, Gar, Bio, Epi, are generally present in various combinations only in small amounts or may be absent. Bulk CFM compositions

cluster around the composition of hornblende. That this is so in general is suggested by the fact that the compositions of average basalts, the protolith for many amphibolites, project near the hornblende line in Figure 1. Parts of the projected CFM liquidus relationships for subfacies 6 and 7 are illustrated in Figure 4. The liquidus relationships were determined on the basis of assumptions presented by Abbott and Clarke (1979) and Abbott (1981). Briefly, the following assumptions were made. (1) Each CFM topology in Figure 3 may be considered the Alkemade relationships for melting in the corresponding subfacies. For every 2-mineral and 3-mineral CFM assemblage there must be a corresponding liquidus equilibrium which is the locus of the liquids coexisting with the 2- or 3-mineral assemblages respectively. The 3-phase equilibria (2 mineral + liquid) and 4-phase equilibria (3 mineral + liquid) may be odd or even, using the terminology of Ricci (1951), depending on the projected composition of the liquid. The odd-even ambiguity is reconciled in the following ways. (2) The ratio of F/M is always higher in the liquid than in the coexisting mineral assemblage. (3) All liquids in the CFM projection proceed, during ideal fractional crystallization, to one minimum, which according to assumption 2 must be on the CF join. (4) The lowest temperature on the liquidus surface is in the peraluminous part of the CFM projection ($C < 0$). The natural counterparts for petrogeny's residual system, pegmatites and highly differentiated granites, are almost always peraluminous, even when earlier rocks in a differentiated series are subaluminous or metaluminous.

It was argued by Abbott (1981) that part of the primary liquidus field for hornblende extends into the peraluminous region, where, for instance, the 3-phase CFM equilibrium Liq + Bio + Hnb would be odd such that Liq + Hnb = Bio. The 4-phase CFM equilibrium Liq + Bio + Hnb + Gar is also in the peraluminous region and this has an important bearing on anatexis of many of the metabasites in the Ashe Formation because the first liquid will appear at the liquidus point marking this equilibrium. Other 'first' liquids may appear on the Gar + Hnb + Liq liquidus line or at the point marking the Gar + Hnb + Epi + Liq equilibrium, depending on the initial mineral assemblage. With regard to subfacies 6, if part of the hornblende liquidus field extends into the peraluminous region, the 4-phase equilibrium Epi + Hnb + Bio + Liq is most likely odd and in the peraluminous region. *The first liquid to appear in subfacies 6* (*e.g.*, in the Ashe Formation) *will appear at the 4-phase equilibrium, hence will be peraluminous.*

The CFM liquidus surface, or parts thereof, as in Figure 4, can be postulated for any of the other CFM topologies in Figure 3, on the basis of the assumptions outlined above.

The high grade metabasite terranes, such as the Ashe Formation which, along with presumed equivalents, underlies much of the Blue Ridge Province in the southern Appalachian Orogen, could have been fertile ground for the generation of impressive amounts of peraluminous, granitic magma. Large volumes of granitic magma may not have been removed from the Ashe Formation. Elsewhere large scale mobilization may have taken place from terranes now exposed at the surface or still buried deep in the crust.

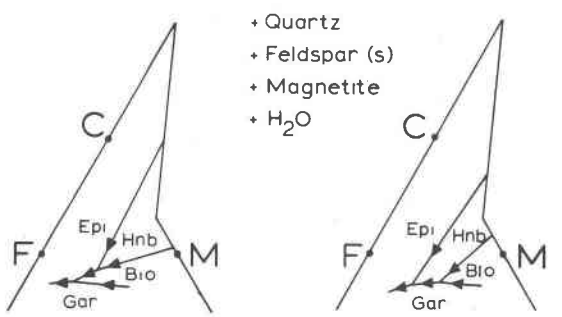

Fig. 4. Partial CFM liquidus projections consistent with parts of the CFM subsolidus topologies of subfacies 5 (or 6) and subfacies 7 (or 9). The arrows on the loci of liquids in 3-phase equilibria (2 minerals + liquid) indicate the direction of falling temperature.

Conclusions

The petrogenetic grid presented here should be helpful in the qualitative assessment of the grade of metamorphism in metabasites. Details of the grid will change as new information becomes available. There is a need to identify additional natural mineral assemblages in high temperature–low pressure terranes. Felsic volcanic and plutonic rocks may be of use in this regard, particularly for interpreting the high F/M relationships.

The CFM relationships provide a direct link with relationships in pelitic systems ($C < 0$). The correlation between metabasite assemblages discussed in this paper and metapelitic assemblages has yet to be adequately treated.

Acknowledgments

I am grateful for the reviews and comments of Loren A. Raymond, Harry Y. McSween and Jo Laird. Financial support for this paper was provided by Appalachian State University.

References

Abbott, R. N., Jr. (1981) AFM liquidus projections for granitic magmas, with special reference to hornblende, biotite and garnet. Canadian Mineralogist, 19, 103–110.

Abbott, R. N., Jr. and Clarke, D. B. (1979) Hypothetical liquidus relationships in the subsystem Al_2O_3–FeO–MgO projected from quartz, alkali feldspar and plagioclase for $a(H_2O) \leq 1$. Canadian Mineralogist, 17, 549–560.

Albee, A. L. (1965) A petrogenetic grid for the Fe–Mg silicates of pelitic schists. American Journal of Science, 263, 512–536.

Bacon, C. R. and Duffield, W. A. (1981) Late Cenozoic rhyolites from the Kern Plateau, southern Sierra Nevada, California. American Journal of Science, 281, 1–34.

Benson, W. N. (1941) Cainozoic petrographic provinces of New Zealand. American Journal of Science, 239, 537–552.

Bird, D. K. and Helgeson, H. G. (1981) Chemical interaction of aqueous solutions with epidote-feldspar mineral assemblages in geologic systems. II Equilibrium constraints in metamorphic/geothermal processes. American Journal of Science, 281, 576–614.

Coleman, R. C., Lee, D. E. and Brannock, W. W. (1965) Eclogites and eclogites, their differences and similarities. Geological Society of America Bulletin, 76, 483–508.

Dobretsov, N. L., Khlestov, V. V. and Sobolev, V. S. (1972) The Facies of Regional Metamorphism at Moderate Pressures. (transl. D. A. Brown, Australian National University, Canberra, 1973).

Engel, A. E. J. and Engel, C. G. (1962) Progressive metamorphism of amphibolite, northwest Adirondack Mountains, New York. Geological Society of America, Buddington Volume, 37–82.

Ernst, W. G. (1968) Amphiboles. Springer-Verlag, New York.

Eskola, P. (1939) Die Enstehung der Gesteine. Springer, Berlin.

Eugster, H. P. (1956) Stability of hydrous iron silicates. Annual Report of the Director of the Geophysical Laboratory, Carnegie Institute of Washington Yearbook, 55, 158–161.

Eugster, H. P. and Wones, D. R. (1962) Stability relations of the ferruginous biotite, annite. Journal of Petrology, 3, 82–125.

Ferry, J. M. (1978) Fluid interaction between granite and sediment during metamorphism, south-central Maine. American Journal of Science, 278, 1025–1056.

Ferry, J. M. (1979) Reaction mechanisms, physical conditions, and mass transfer during hydrothermal alteration of mica and feldspar in granitic rocks from south-central Maine, U.S.A. Contributions to Mineralogy and Petrology, 68, 125–139.

Harte, B. and Graham, G. M. (1975) The graphical analysis of greenschist to amphibolite facies mineral assemblages in metabasites. Journal of Petrology, 16, 347–370.

Jan, M. Q. and Howie, R. A. (1981) The mineralogy and geochemistry of the metamorphosed basic and ultrabasic rocks of the Jijal Complex, Kohistan, NW Pakistan. Journal of Petrology, 22, 85–126.

Johannsen, A. (1939) A Descriptive Petrography of the Igneous Rocks. University of Chicago Press, Chicago.

Jones, T. Z. (1973) Petrography, Structure, and Metamorphic History of the Warrensville and Jefferson Quadrangles, Southern Blue Ridge, Northwestern North Carolina. Ph.D. Thesis, Miami University, Ohio.

Kay, R. W. and Kay, S. M. (1981) The nature of the lower continental crust: Inferences from geophysics, surface geology, and crustal xenoliths. Reviews in Geophysics and Space Physics, 19, 271–297.

Klein, C., Jr. (1968) Coexisting amphiboles. Journal of Petrology, 9, 281–330.

Korzhinskii, D. S. (1936) Paragenetic analysis of quartz-containing, almost calciumless crystalline schist of the Archean complex to the south of Baikal Sea. Zapiski Vsesoyuznogo Mineralogicheskogo Obshchestva, 2, 247–280. (not seen; extracted from; J. A. Grant, American Journal of Science, 273, 289–317, 1973).

Korzhinskii, D. S. (1957) Physicochemical Basis of the Analysis of the Paragenesis of minerals. (translated from Russian, Consultants Bureau, Inc., New York, 1959).

Kushiro, I. (1970) Stability of amphibole and phlogopite in the upper mantle. Annual Report of the Director of the Geophysical Laboratory, Carnegie Institute of Washington Yearbook, 68, 245–247.

Laird, J. (1980) Phase equilibria in mafic schist from Vermont. Journal of Petrology, 21, 1–37.

Liou, J. G. (1973) Synthesis and stability relations of epidote, Ca_2Al_2Fe–$Si_3O_{12}(OH)$. Journal of Petrology, 14, 381–413.

MacDonald, G. A. (1949) Petrography of the island of Hawaii. U.S. Geological Survery Professional Paper 214-D.

Oyawaye, M. O. and Makanjaola, A. A. (1972) Bauchite: A fayalite-bearing quartz monzonite. International Geological Congress, 24th Session, Section 2, Petrology, Montreal, 251–266.

Rankin, D. W., Espenshade, G. H. and Newman, R. B. (1972) Geological map of the west half of the Winston-Salem quadrangle, N.C., Va., Tenn. U.S. Geological Survey Miscellaneous Geological Investigations, Map I-709A.

Rankin, D. W., Espenshade, G. H. and Shaw, K. W. (1973) Stratigraphy and structure of the metamorphic belt in northwestern North Carolina and southwestern Virginia: A study from the Blue Ridge across the Brevard Fault Zone to the Sauratown Mountains Anticlinorium. American Journal of Science, Cooper Volume 273-A, 1–40.

Reinhardt, E. W. and Skippen, G. B. (1970) Geological Survey of Canada Report of Activities, Paper 70-1, part B, 48–54.

Ricci, J. E. (1951) The Phase Rule and Heterogeneous Equilibrium. Van Nostrand, New York.

Robinson, P. and Jaffe, H. W. (1969) Aluminous enclaves in gedrite-cordierite gneiss from southwestern New Hampshire. American Journal of Science, 267, 389–421.

Ronov, A. B. and Yaroshevsky, A. A. (1969) Chemical compositions of the earth's crust. In P. J. Harte, Ed., The Earth's Crust and Upper Mantle, p.37–57. American Geophysical Union Monograph 13, Washington.

Spear, F. S. (1981) An experimental study of hornblende stability and compositional variability in amphibolite. American Journal of Science, 281, 697–734.

Thompson, J. B., Jr. (1957) The graphical analysis of mineral assemblages in pelitic schists. American Mineralogist, 42, 842–858.

Turner, F. J. (1948) Mineralogical and Structural Evolution of the Metamorphic Rocks. Geological Society of America Memoir 30.

Turner, F. J. (1968) Metamorphic Petrology. McGraw-Hill, New

York.

Tuttle, O F. and Bowen, N. C. (1958) The Origin of Granite in the Light of Experimental Studies in the System $NaAlSi_3O_8$–$KalSi_3O_8$–SiO_2–H_2O. Geological Society of America Memoir 74.

Washington, H. S. (1922) Deccan traps and other plateau basalts. Journal of Geology, 33, 765–804.

Wentworth, C. K. and Winchell, H. (1947) Koolau basalt series, Oahu, Hawaii. Geological Society of America Bulletin, 58, 49–78.

Windley, B. F. (1970) Primary ferro-dolerite/garnet amphibolite dykes in the Sukkertoppen region of west Greenland. In G. Newall and N. Rast, Eds., p. 79–92. Mechanism of Igneous Intrusion, Geological Journal Special Issue, 2.

Winkler, H. G. F. (1965) Petrogenesis of Metamorphic Rocks. Springer, Berlin.

Winkler, H. G. F. (1979) Petrogenesis of Metamorphic Rocks. 5th Edition. Springer, New York.

Yoder, H. S. and Eugster, H. P. (1954) Phlogopite synthesis and stability range. Geochimica et Cosmochimica Acta, 6, 179–182.

Manuscript received, December 18, 1981;
accepted for publication, May 3, 1982.